Laser-Controlled Torsions: Four-Dimensional Theory and the Validity of Reduced Dimensionality Models

Thomas Grohmann, Monika Leibscher, and Tamar Seideman

Laser-controlled torsions: a four-dimensional theory and the validity of reduced dimensionality models

Thomas Grohmann,[1] Monika Leibscher,[2] and Tamar Seideman[1]

[1]*Department of Chemistry, Northwestern University,*
2145 Sheridan Rd, Evanston, Illinois 60208, USA
[2]*Institut für Theoretische Physik, Leibniz Universität Hannover, Appelstr. 2, Hannover, Germany*
(Dated: April 10, 2017)

A multitude of possible applications along with unique coherence, chirality and symmetry properties makes the control of molecular torsion with moderately strong, non-resonant laser pulses a fascinating subject. A description of combined rotation and torsion requires at least four angular degrees of freedom, which is challenging for the majority of systems. Lower-dimensional models have been proposed but also questioned. Here, we develop a four-dimensional model for the coupled rotational-torsional motions of molecules consisting of two identical moieties. By comparing four-dimensional calculations with a two-dimensional model, we define conditions under which the lower-dimensional model is valid. In particular, we point to the crucial role of coordinate dependence of the polarizability tensor. Our results do not agree with those of previous four-dimensional calculations, but support the conclusions of recent experiments.

The ability to control the torsions of non-rigid molecules has been fascinating theoretical chemists and molecular physicists for several decades. Among the variety of applications of torsional control that have fueled this interest are the control of energy transfer [1], charge transport [2] and chemical reactions [3], the enhancement of transient absorption spectroscopy [4] and the design of molecular rotors [5–7]. A relatively recent approach to manipulating the conformation of molecules in the electronic ground state involves the application of a moderately intense, non-resonant laser field to generate a broad torsional wavepacket that is correspondingly localized in the conjugated angle space. This approach was first proposed in 2007 [8] and later explored in more detail in several theoretical and experimental studies [7, 9–12]. Extending these ideas, many interesting topics have been studied, including the interconversion of enantiomeres of axially chiral molecules [4, 13], nuclear spin selective control of molecular torsion [6] and torsional alignment in a dissipative environment [14].

As the interaction with non-resonant laser fields couples the molecular torsion with rotation, at least four coordinates are necessary to characterize the molecular motion—the three Euler angles, θ, ϕ, χ, and one coordinate ρ describing intramolecular torsion. The high numerical effort of accounting for four coupled angular modes led to the application of low-dimensional models in the vast majority of theoretical studies on torsional control, presupposing a two-step mechanism to be valid: A nanosecond laser pulse aligns the principal molecular axis, before a second, femtosecond laser pulse selectively excites molecular torsion, see Fig. 1. Several experimental studies suggest the validity of this model [7, 10–12]. Yet, strong doubts have been expressed concerning the possibility to control torsions separately from the rotational modes [15–17]. Quantum dynamical simulations for single-pulse excitations suggested that the

torsional dynamics strongly depends on the overall rotation and hence the torsional alignment predicted by low-dimensional models is completely destroyed due to rotational-torsional couplings [15, 17].

Given the results of [15–17], the growing experimental interest in the strong field torsional control approach [7, 10–12] and the large variety of applications of torsional control [9], it is important to revisit this problem with reliable calculations. In particular, since the many applications depend on the assumption that torsional alignment does not disappear due to coupling to rotational degrees of freedom. In the present work we perform fully quantum, four-dimensional (4D) calculations of torsional alignment that question the conclusions of [15–17]. We point to, and physically explain, the role played by the coordinate dependence of the polarizability tensor. By comparing the 4D with the two-dimensional (2D) approach to torsional control, we suggest that the reliability of 2D simulations is closely related to the quality of the additive model, commonly used in strong-field control for describing molecular polarizabilities. Moreover, we illustrate that the rotational-torsional coupling can be effectively controlled by appropriately choosing the laser parameters.

As in earlier works [15–17], we consider molecules in which the two molecular subunits undergoing mutual torsion are identical. In particular, we exemplify our arguments for diboron tetrafluoride (B_2F_4) and 4,4'-Dibromobiphenyl (DBBP); two very different molecules in what regards their torsional structure, rotational constants and polarizability anisotropy, which together are expected to represent many chemically interesting molecules. We limit our discussion to states having the symmetry of the field-free rotational-torsional ground states [15–19].

The complete Hamiltonian for the two-pulse scenario illustrated in Fig. 1 is given by $\hat{H} = \hat{H}^{\text{rt}} + \hat{H}_1^{\text{int}} + \hat{H}_2^{\text{int}}$,
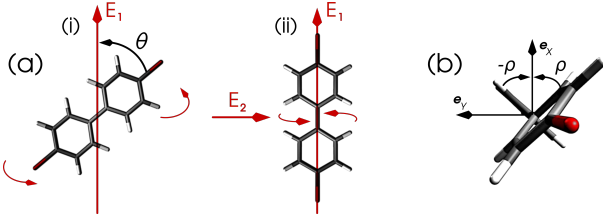
FIG. 1. (a) *Excitation scheme:* (i) A nanosecond pulse, E_1, adiabatically aligns the most polarizable molecular axis. (ii) A second, femtosecond pulse, E_2, polarized perpendicular to the first pulse excites a rotational-torsional wave packet. The angle between the molecular axis and the external field E_1 is θ. (b) *Torsion angle:* The torsion angle ρ is half of the dihedral angle between the two moieties of the molecule.

consisting of the field-free rotational-torsional Hamiltonian $\hat{H}^{\mathrm{rt}}$ and the Hamiltonians describing the field-matter interaction $\hat{H}_i^{\mathrm{int}}$. The field-free term $\hat{H}^{\mathrm{rt}}$ reads [19]

$$
\hat{H}^{\mathrm{rt}} = \mathfrak{B}_{X^2+Y^2}\left(\hat{J}_X^2 + \hat{J}_Y^2\right) + \mathfrak{B}_{X^2-Y^2}\left(\hat{J}_X^2 - \hat{J}_Y^2\right) \\
+ \mathfrak{A}\left(\hat{J}_Z^2 + \hat{J}_\rho^2\right) + V^{\mathrm{tor}}(\rho) ,
$$

(1)

with

$$
\mathfrak{B}_{X^2+Y^2}(\rho) = \mathfrak{B}\,\frac{1}{1 - \mathfrak{B}_{\mathrm{red}}^2 \cos^2(2\rho)} \\
\mathfrak{B}_{X^2-Y^2}(\rho) = \mathfrak{B}\,\frac{\mathfrak{B}_{\mathrm{red}}\cos(2\rho)}{1 - \mathfrak{B}_{\mathrm{red}}^2 \cos^2(2\rho)} .
$$

(2)

In Eq. (1), $\mathfrak{A}$ is the rotational constant associated with the torsional axis, and $\mathfrak{B}$ is the rotational constant perpendicular to the molecular axis for $2\rho = \{90°, 270°\}$. Both constants and the torsional potential V^{tor} of the electronic ground-state we calculate using density functional theory [26]. Since the rotational functions in Eq. (2) depend on ρ, the rotations and torsion are coupled in the field-free case. The magnitude of the effective coupling $\mathfrak{B}_{X^2\pm Y^2}/\mathfrak{B}$ is completely determined by the reduced rotational constant $\mathfrak{B}_{\mathrm{red}} = \mathfrak{B}/2\mathfrak{A}$. For $\mathfrak{B}_{\mathrm{red}} \to 0$, the coupling vanishes and the rotational-torsional Hamiltonian $\hat{H}^{\mathrm{rt}}$ is a separable function of the Hamiltonian of a symmetric top and the pure torsional Hamiltonian.

The Hamiltonians for the field-matter interaction can be written as [20]

$$
\hat{H}_i^{\mathrm{int}} = -\frac{1}{4}|\epsilon_i(t)|^2 \alpha_{qq} ,
$$

(3)

where $\epsilon_i(t)$ is the envelope of laser pulse $E_i(t)$. We choose $q = z$ and x for the polarization directions of the first and second pulse, respectively. We express the laboratory-fixed components of the molecular polarizabilities

$$
\alpha_{zz} = \frac{\alpha^{(0,0)}}{\sqrt{3}} + \frac{2\,\alpha^{(2,0)}}{\sqrt{6}}\mathcal{D}_{0,0}^2 + \frac{\alpha^{(2,2)}}{\sqrt{3}}\left(\mathcal{D}_{0,2}^2 + \mathbf{c.c.}\right)
$$

$$
\alpha_{xx} = \frac{\alpha^{(0,0)}}{\sqrt{3}} - \frac{2\alpha^{(2,0)}}{\sqrt{6}}\left[\mathcal{D}_{0,0}^2 - \frac{3}{\sqrt{6}}\left(\mathcal{D}_{2,0}^2 + \mathbf{c.c.}\right)\right] \quad (4)
$$

$$
- \frac{\alpha^{(2,2)}}{\sqrt{2}}\left[\frac{1}{\sqrt{6}}\mathcal{D}_{0,2}^2 - \frac{1}{2}\left(\mathcal{D}_{2,2}^2 + \mathcal{D}_{2,-2}^2\right) + \mathbf{c.c.}\right]
$$

in terms of the elements of the Wigner D-matrices $\mathcal{D}_{m,k}^J$ [21] and the symmetry-adapted, molecule-fixed components of the polarizability tensor [18] $\alpha^{(0,0)}$, $\alpha^{(2,0)}$ and $\alpha^{(2,2)}$. For molecules with feasible torsion, the latter depend on the torsion angle ρ, resulting in a second, field-induced type of rotational-torsional coupling. A reliable description of the ρ-dependence is thus essential to understand this kind of coupling. Due to their symmetry, we can write the components of the polarizability tensor as

$$
\alpha^{(J,K)}(\rho) \approx \alpha_0^{(J,K)} \sum_{n=0}^N \mathcal{A}_n^{(J,K)} \cos((4n+K)\rho) .
$$

(5)

Here, $(J,K) = \{(0,0),(0,2),(2,2)\}$, $\alpha_0^{(J,K)} \equiv \alpha^{(J,K)}(\rho = 0)$, and $\mathcal{A}_n^{(J,K)}$ are expansion coefficients we determine numerically. Our quantum chemical calculations show that for the systems we consider here, $N = 2$ is sufficient to describe the ρ-dependence of the polarizabilities [26]. Using Eq. (5), we go beyond the majority of theoretical approaches to torsional control, which make use of the additive model for molecular polarizabilities. The additive model expresses the polarizabilities of the molecule as sums of the polarizabilities of the molecular subunits [22], which is identical to setting $N = 0$ in Eq. (5).

In a 2D description, we premise that the principal molecular axis is perfectly aligned to the laboratory-fixed z-axis, as depicted in panel (ii) in Fig. 1(a). The remaining coordinates are the Euler angle χ and the torsion angle ρ. Formally, we obtain the 2D Hamiltonian by calculating the limit $\theta \to 0$ and $\phi \to 0$ in Eqs. (1), (3) and (4). Within the 2D approach to torsional control the field-free coupling therefore vanishes.

To quantify their interaction with the nanosecond pulse, we assume that the molecules are initially in their rotational-torsional ground state and adiabatically transform into the ground state of the field-dressed Hamiltonian $\hat{H}^{\mathrm{fd}} \equiv \hat{H}^{\mathrm{rt}} + \hat{H}_1^{\mathrm{int}}$. We compute these "pendular states" [23] by calculating the eigensystem of $\hat{H}^{\mathrm{fd}}$ using a variational procedure with tensor-products of the symmetric top and torsional states as a basis. The interaction with the femtosecond pulse then creates a rotational-torsional wave packet that can be written as a superposition of pendular states. As the pulse is short compared to the rotational-torsional dynamics, we can employ the impulsive approximation [6, 24] to obtain the expansion coefficients in that superposition. To quantify the degree
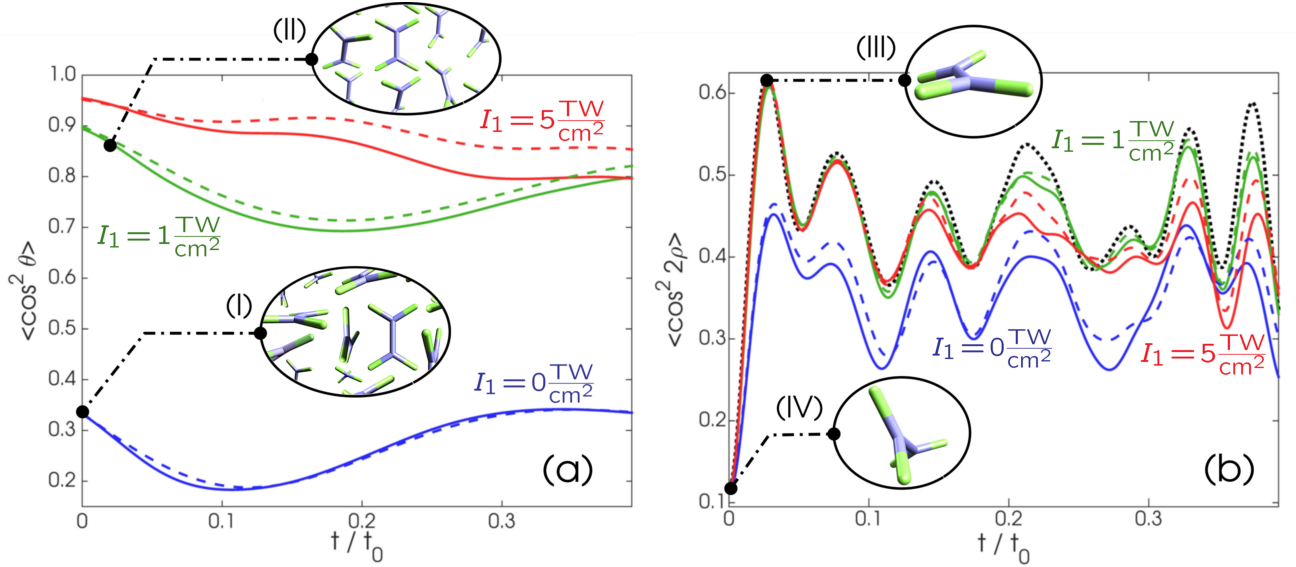
FIG. 2. Alignment factors $\langle\cos^2\theta\rangle$ (a) and $\langle\cos^2 2\rho\rangle$ (b) of B_2F_4 after interaction with an x-polarized pulse with intensity $I_2 = 50\,\mathrm{TW\cdot cm^{-2}}$ and duration $\tau = 150$ fs. The solid curves display the results of 4D simulations in the presence of a z-polarized nanosecond pulse with $I_1 = 0, 1, 5\,\mathrm{TW\cdot cm^{-2}}$ (blue, green and red curves online). The dashed lines represent the same simulations without field-free rotational-torsional coupling. 2D simulations are depicted in dotted lines in panel (b). Time is given in units of $t_0 = \hbar/\mathfrak{A} = 30$ ps. For all 4D simulations $J_{\max} = 20$. The cartoons illustrate the classical interpretation of the respective alignment factor: the molecules are completely randomly (I) or almost perfectly (II) aligned to the polarization direction of the first laser pulse; B_2F_4 shows almost perfect (III) or almost no (IV) torsional alignment.

of rotational and torsional control, we calculate the alignment factor for the torsion $\langle\cos^2 2\rho\rangle$ and the alignment of the principal axis with respect to the polarization of the first laser pulse $\langle\cos^2\theta\rangle$. The former factor is equal to one (zero), if the two parts of the molecule are coplanar (twisted by 90°); the alignment factor $\langle\cos^2\theta\rangle$ is one (zero), if the molecule is perfectly aligned (orthogonal) to the polarization of the first laser pulse. Per definition, in the 2D model, $\langle\cos^2\theta\rangle \equiv 1$.

As a first example, we investigate the rotational-torsional dynamics of B_2F_4, which has a low effective torsional barrier and a potential minimum at $2\rho \approx 70°$ [26]. Figure 2 shows the rotational alignment factor $\langle\cos^2\theta\rangle$ (a) and the torsional alignment factor $\langle\cos^2 2\rho\rangle$ (b) for B_2F_4 after excitation with a short, x-polarized laser pulse within the 4D (colored lines) and 2D (dotted line) approaches. In all cases, we observe a considerable increase of the torsional alignment immediately after the interaction: the small torsional barrier and the initially twisted geometry of B_2F_4 promote excitation of torsional motion [6]. In the absence of the nanosecond pulse, the molecular axis is not aligned, the angular distribution of the molecules remains isotropic, as indicated in oval (I) in Fig. 2 (a). Here, the degree of torsional alignment is reduced compared to the 2D model. In the presence of a nanosecond pulse (green and red lines), however, the molecular axis is well aligned, and the initial torsional dynamics is in very good agreement with the 2D model.

For B_2F_4, our calculations thus support what recent

experiments have illustrated: the adiabatic pulse effectively transforms the motion to two-dimensional, simplifying the multimode dynamics and allowing for the selective control of the torsion [7, 10–12]. For $I_1 = 1\,\mathrm{TW\cdot cm^{-2}}$ (green lines), the good agreement between 2D and 4D simulations continues during the later stage of the time-evolution. Hence, in case of moderately strong adiabatic fields, our simulations justify a 2D description of the rotational-torsional dynamics, and a "breakdown of torsional quantum control", as observed in earlier simulations [15–17], does not occur. For a stronger adiabatic field (red line), the results are less intuitive: although the agreement between the two models is excellent for short time scales, the 2D model does not fully account for the dephasing that the 4D model exhibits as time evolves. Similar non-monotonous behavior has been observed earlier in the dynamics of rotational and torsional wavepackets [6, 24, 25].

Our second example, DBBP, displays very different rotational-torsional dynamics, as we show in Fig. 3. In order to simplify the comparison of the two molecules, we reduce the effective barrier of DBBP to that of B_2F_4 and adjust the laser intensities. First, we find that the alignment factor $\langle\cos^2\theta\rangle$ is almost constant in time. Thus, the alignment of the principal molecular axis and the rotational-torsional dynamics perpendicular to it are separated since they occur on different time scales. Without the nanosecond pulse (blue lines), $\langle\cos^2\theta\rangle \approx 1/3$, i.e. the angular distribution of molecules is almost isotropic,
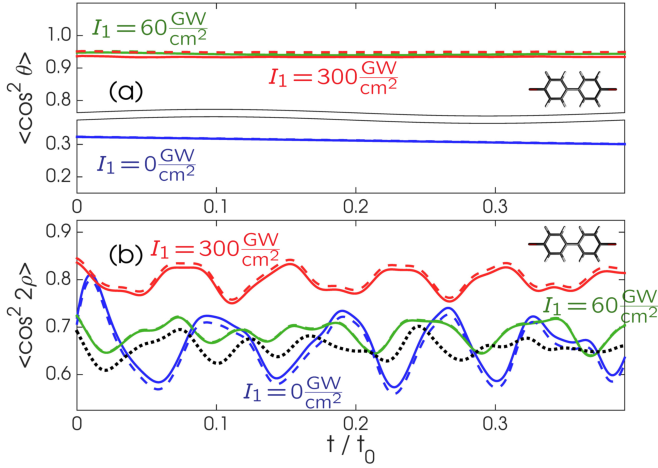
FIG. 3. Alignment factors $\langle \cos^2 \theta \rangle$ (a) and $\langle \cos^2 2\rho \rangle$ (b) of DBBP after interaction with a x-polarized pulse of intensity $I_2 = 5.6\,\mathrm{TW\cdot cm^{-2}}$ and duration $\tau = 150$ fs. The solid curves display the results of 4D simulations in the presence of a z-polarized nanosecond pulse with $I_1 = 0, 60, 300\,\mathrm{GW\cdot cm^{-2}}$ (blue, green and red curves online). The dashed lines represent the same simulations without field-free rotational-torsional coupling. 2D simulations are depicted in dotted lines in panel (b). Time is given in units of $t_0 = \hbar/\mathfrak{A} = 50$ ps. For all 4D simulations $J_{\max} = 20$.

FIG. 4. *Left:* Torsional alignment factor $\langle \cos^2 2\rho \rangle$ for B_2F_4 (upper panel) and DBBP (lower panel) after interaction with the second laser pulse with intensity $I_2 = 50\,\mathrm{TW\cdot cm^{-2}}$ for B_2F_4 and $I_2 = 5.6\,\mathrm{TW\cdot cm^{-2}}$ for DBBP; $\tau = 150$ fs in both cases. For the intensity of the nanosecond pulse we chose $I_1 = 1\,\mathrm{TW\cdot cm^{-2}}$ for B_2F_4 and $I_1 = 300\,\mathrm{GW\cdot cm^{-2}}$ for DBBP. Time is given in units of $t_0 = \hbar/\mathfrak{A} = 30$ ps for B_2F_4 and $t_0 = \hbar/\mathfrak{A} = 50$ ps for DBBP. *Right:* ρ-dependence of the polarizabilities $\alpha^{(0,0)}/\alpha_0^{(0,0)}$ (top), $\alpha^{(2,0)}/\alpha_0^{(2,0)}$ (middle) and $\alpha^{(2,2)}/\alpha_0^{(2,2)}$ (bottom) for B_2F_4 (upper panel) and DBBP (lower panel). In case they are distinguishable, calculations with the full form of the polarizabilities (blue lines online) are marked with qc, calculations using the additive model (brown lines online) with am; 2D simulations using the additive model are illustrated by dotted lines.

while a moderately intense nanosecond pulse (green lines) almost perfectly aligns the molecules. For DBBP, however, pre-alignment does not lead to better torsional alignment. Here, it is the isotropic angular distribution (blue lines) that promotes extended torsional dynamics and alignment. Analogously to B_2F_4, the simulations from the 2D model (dotted lines in Fig. 3) agree best with the 4D simulations if the nanosecond pulse is of moderate intensity (green line in Fig. 3). Yet, the two curves are shifted: at t=0, the green curve already shows a slightly larger amount of torsional alignment. This is because for DBBP, the lowest field-dressed state contains contributions from excited torsional states, which are not accounted for in the 2D model. The effect is even more pronounced with increasing intensity of the nanosecond pulse, as the red curves in Fig. 3 (b) show.

To unravel the mechanisms responsible for the complex torsional dynamics illustrated in Figs. 2 and 3, we calculated the alignment factors without field-free coupling; these results are depicted in dashed lines in Figs. 2 and 3. For B_2F_4 ($\mathfrak{B}_{\mathrm{red}} = 0.19$), comparison with the calculations including the full coupling (solid lines in Fig. 2) shows that the field-free coupling slightly reduces the torsional and rotational alignment. However, the effect is too small to account for the differences between 2D and 4D simulations. For DBBP ($\mathfrak{B}_{\mathrm{red}} = 0.015$), Fig. 3, the field-free rotation-torsion coupling has practically no influence on the alignment, neither for the torsion nor the rotatio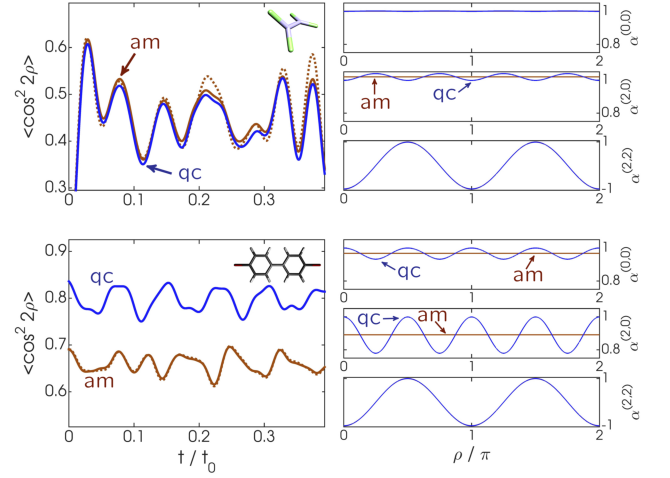n. We conclude that in general the effect of field-free rotation-torsion couplings on torsional alignment is comparatively small and the more important source of torsion-rotation interaction is the field-induced coupling, expressed by the polarizabilities of Eq. (4).

We can underline our argument by scrutinizing a further assumption made in most of the past studies: the additive model for the molecular polarizabilities. Within the additive model, only the component $\alpha^{(2,2)}$ depends on ρ, while $\alpha^{(0,0)}$ and $\alpha^{(2,0)}$ are considered to be constant, minimizing the field-induced rotational-torsional coupling, *c.f.* Eq. (5). In Fig. 4, the ρ-dependence of the polarizability is depicted for the two examples B_2F_4 and DBBP. For B_2F_4 the additive model is a good approximation, while for DBBP the terms $\alpha^{(0,0)}$ and $\alpha^{(2,0)}$ differ considerably from the additive model. Intuitively, this result is expected: molecules with large conjugated π-systems at the coplanar configuration, such as substituted biphenyls, have much greater polarizability anisotropies than smaller molecules like B_2F_4. Yet, as this conjugation is lost at the twisted conformation, their polarizability also depends more strongly on the torsion angle. Consequently, as shown in Fig. 4, for DBBP we observe a considerable difference between simulations employing the additive model (brown line) and ones ac-

counting for the full (blue line) ρ-dependence already at $t = 0$, while for B_2F_4 (upper panel) there is almost no difference. Importantly, the correct coordinate dependence of the polarizability tensor effectively increases the interaction term and hence improves the torsional alignment as compared to past work where the additivity approximation was invoked. From Fig. 4 we also learn that the validity of the 2D model and the additive model correlates: Considering B_2F_4, the results of the 4D simulations with accurate polarizabilities and subject to the additive model, along with the 2D simulations based on the additive model almost coincide. For DBBP, the 4D and 2D simulations lead to practically identical results if the additive model is applied (see solid and dashed brown lines in the lower panel of Fig. 4), while with the complete polarizability the 4D and 2D simulations lead to very different torsional alignment factors, see also Fig. 3 (b). Thus, for most molecules, an accurate description of the molecular polarizabilities beyond the additive model is crucial to predict the rotational-torsional dynamics.

Summarizing, we performed fully quantum, 4D calculations of torsional control and used them to (1) illustrate the critical role played by proper description of the polarizability coordinate-dependence, neglected in past studies; (2) explain that rotation-torsion coupling, in particular field-induced coupling, does not destroy torsional alignment as argued in the past but rather typically assists it; and (3) show how and why the validity of low-dimensional models depends on the choice of the molecule and laser parameters. Because the relevant coupling between rotations and torsions is field-induced, rather than field-free, it can be steered by choosing the polarizations and intensities of the laser fields. We therefore do not believe that temperature is as significant for deciding whether 2D models are reliable approximations as earlier studies have claimed it is [15–17]. Due to the high computational cost of full-dimensional simulations, the study of many applications of torsional alignment will continue to rely on low-dimensional models. Our investigations show that such models are qualitatively correct and suggest that their quantitative accuracy, if necessary, could be enhanced by adiabatic separation of the fast and slow degrees of freedom.

[1] S. Westenhoff, W. J. D. Beenken, R. H. Friend, N. C. Greenham, A. Yartsev, V. Sundström, Phys. Rev. Lett. **97**, 166804 (2006).
[2] M. G. Reuter, M. Sukharev, T. Seideman, Phys. Rev. Lett. **101**, 208303 (2008).
[3] N. T. Anh, Topics in Current Chem. **88**, 145 (1980).
[4] S. M. Parker, M. A. Ratner, T. Seideman, Mol. Phys. **110**, 1941 (2012).
[5] Y. Fujimura, L. González, D. Kröner, J. Manz, I. Mehdaoui, B. Schmidt, Chem. Phys. Lett. **386**, 248 (2004).
[6] J. Floß, T. Grohmann, M. Leibscher, T. Seideman, J. Chem. Phys. **136**, 084309 (2012).
[7] L. Christensen, J. H. Nielsen, C. B. Brandt, C. B. Madsen, L. B. Madsen, C. S. Slater, A. Lauer, M. Brouard, M. P. Johansson, B. Shepperson, H. Stapelfeldt, Phys. Rev. Lett. **113**, 073005 (2014).
[8] S. Ramakrishna and T. Seideman, Phys. Rev. Lett. **99**, 103001 (2007).
[9] B. Ashwell, S. Ramakrishna, S. Seideman, J. Chem. Phys. **138**, 044310 (2013).
[10] C. B. Madsen, L. B. Madsen, S. S. Viftrup, M. P. Johansson, T. B. Poulsen, L. Holmegaard, V. Kumarappan, K. A. Jorgensen, and H. Stapelfeldt, Phys. Rev. Lett. **102**, 073007 (2009).
[11] C. B. Madsen, L. B. Madsen, S. S. Viftrup, M. P. Johansson, T. B. Poulsen, L. Holmegaard, V. Kumarappan, K. A. Jorgensen, and H. Stapelfeldt, J. Chem. Phys. 130, 234310 (2009).
[12] J. L. Hansen, J. H. Nielsen, C. B. Madsen, A. T. Lindhardt, M. P. Johansson, T. Skrydstrup, L. B. Madsen, H. Stapelfeldt, J. Chem. Phys. **136**, 204310 (2012).
[13] S. M. Parker, M. A. Ratner, T. Seideman, J. Chem. Phys. **135** 224301 (2011).
[14] B. Ashwell, S. Ramakrishna, T. Seideman, J. Phys. Chem. C **117**, 22391 (2013).
[15] L. H. Coudert, L. F. Pacios, J. Ortigoso, Phys. Rev. Lett. **107**, 113004 (2011).
[16] J. Ortigoso, L. H. Coudert, Phys. Rev. A **87**, 043403 (2013).
[17] L. H. Coudert, Phys. Rev. A **91**, 013402 (2015).
[18] P. R. Bunker, P. Jensen, *Molecular Symmetry and Spectroscopy, 2nd Edition* (Ottawa, National Research Council of Canada, 1998).
[19] A. J. Merer, J. K. G. Watson, J. Mol. Spec. **47**, 499 (1973).
[20] T. Seideman and E. Hamilton, Ad.At.Mol.Opt.Phys. **52**, 289 (2006).
[21] R. N. Zare *Angular momentum: understanding spatial aspects in chemistry and physics* (New York, Wiley, 1988).
[22] K. D. Bonin, V. V. Kresnin, *Electric-dipole polarizabilities of atoms, molecules and clusters* (Singapore, World Scientific, 1997).
[23] B. Friedrich, D. R: Herschbach, Z. Phys. D **18**, 153 (1991).
[24] T. Grohmann, M. Leibscher, J. Chem. Phys. **134**, 204316 (2011).
[25] M. Leibscher, I. Sh. Averbukh, H. Rabitz, Phys. Rev. Lett. **90**, 213001 (2003).
[26] See Supplemental Material [url], which includes Ref. [27].

[27] Y. Shao, L. Fusti-Molnar, Y. Jung, J. Kussmann, C. Ochsenfeld, S. T. Brown, A. T. B. Gilbert, L. V. Slipchenko, S. V. Levchenko, D. P. O'Neill, R. A. DiStasio Jr., R. C. Lochan, T. Wang, G. J.O. Beran, N. A. Besley, J. M. Herbert, C. Yeh Lin, T. Van Voorhis, S. Hung Chien, A. Sodt, R. P. Steele, V. A. Rassolov, P. E. Maslen, P. P. Korambath, R. D. Adamson, B. Austin, J. Baker, E. F. C. Byrd, H. Daschel, R. J. Doerksen, A. Dreuw, B. D. Dunietz, A. D. Dutoi, T. R. Furlani, S. R. Gwaltney, A. Heyden, S. Hirata, C.-P. Hsu, G. Kedziora, R. Z. Khaliullin, P. Klunzinger, A. M. Lee, M. S. Lee, W. Z. Liang, I. Lotan, N. Nair, B. Peters, E. I. Proynov, P. A. Pieniazek, Y. M. Rhee, J. Ritchie, E. Rosta, C. D. Sherrill, A. C. Simmonett, J. E. Subotnik, H. L. Woodcock III, W. Zhang, A. T. Bell, A. K. Chakraborty, D. M. Chipman, F. J. Keil, A. Warshel, W. J. Hehre, H. F. Schaefer III, J. Kong, A. I. Krylov, P. M.W. Gill, M. Head-Gordon, Phys. Chem. Chem. Phys., **8**, 3172 (2006).